National Defence / Défense nationale

RESULTS FROM THE RADAR DIRECTION FINDING FIELD TRIALS HELD AT OSBORNE HEAD IN OCTOBER 1995

by

William Read

DEFENCE RESEARCH ESTABLISHMENT OTTAWA
REPORT NO. 1330

Canada

January 1998
Ottawa

105-02569/

National Defence / Défense nationale

RESULTS FROM THE RADAR DIRECTION FINDING FIELD TRIALS HELD AT OSBORNE HEAD IN OCTOBER 1995

by

William Read
EW Sensors Group
Electronic Support Measures Section

DEFENCE RESEARCH ESTABLISHMENT OTTAWA
REPORT NO. 1330

PROJECT
5BD11

January 1998
Ottawa

ABSTRACT

This report discusses the results of microwave radio direction finding (DF) experiments carried out using the horizontal linear antenna array of an experimental N-channel radar system. The main purpose of these experiments was to investigate the effect of the maritime propagation environment on DF performance for signal paths up to and beyond the radio horizon. As part of this investigation, a comprehensive error analysis was carried out to identify and quantify the most significant sources of bearing error. These sources were mainly instrumental in error although significant errors could also be produced as a result of destructive interference between the direct signal and the ocean surface reflected signal. Based on the error analysis, it was concluded that in a maritime environment, microwave direction finding accuracies of significantly better than one degree RMS are possible, even for paths several kilometers over the radio horizon.

RÉSUMÉ

Le présent rapport traite des résultats d'expériences de radiogoniométrie par ondes hyperfréquences réalisées au moyen de l'antenne réseau rectiligne d'un système radar expérimental à canal N. Ces expériences visaient principalement à étudier, en matière de propagation des ondes, l'incidence du milieu marin sur le trajet des signaux jusqu'à l'horizon radioélectrique et au-delà. Pour les besoins de cette étude, on a effectué une analyse d'erreur exhaustive afin de déterminer et quantifier les sources d'erreur de gisement les plus importantes. Ces sources se sont révélées la principale cause d'erreurs même si des erreurs importantes peuvent aussi résulter de l'interférence destructive entre le signal direct et celui qui est reflété par la surface de l'océan. L'analyse d'erreur a permis de conclure qu'il est possible d'obtenir en milieu marin, grâce à la radiogoniométrie par ondes à hyperfréquences, une précision de plus d'un degré efficace, même pour des trajets de plusieurs kilomètres au-delà de l'horizon radioélectrique.

EXECUTIVE SUMMARY

High accuracy radar direction finding (DF) is a useful feature for a modern ESM system, particularly in view of its potential for improvement in the transmitter identification process as well as the addition of a geolocation capability.

To quantify the benefits of a high accuracy radar DF capability, research and development work has been carried out at the Defence Research Establishment Ottawa (DREO) over the last few years. As part of this work, an investigation was undertaken to determine the effects of the environment on radar DF accuracy. In particular, field trials were carried out in October 1995 at Osborne Head Gunnery Range near Halifax on Canada's East coast to investigate the effects of the maritime propagation environment on the accuracy of measuring the azimuth angle-of-arrival of a radar signal.

During the measurement trials, RMS errors of 0.2 degrees were achieved with the main sources of error being instrumental in nature. Environmental effects were found to be virtually negligible except when cancellation, or near cancellation, of the direct signal by the surface reflected signal occurred. Depending on the heights of the transmitter and receiver, and the distance between them, cancellation occurred up to once every 4 seconds, consistent with half the period of the ocean waves.

Based on these results, it was concluded that high accuracy radar DF (significantly better than 1° RMS) can be achieved in a maritime environment. Although it was found that signal losses rapidly increase beyond the radio horizon, high accuracy DF was still achievable for ranges several kilometers beyond the horizon. By comparison, radar performance degrades more rapidly at these ranges due to a doubling of the signal losses over the two-way radar path.

TABLE OF CONTENTS

	Page
ABSTRACT/RÉSUMÉ	iii
EXECUTIVE SUMMARY	v
TABLE OF CONTENTS	vii
LIST OF FIGURES	ix
LIST OF TABLES	xi
1.0 INTRODUCTION	1
2.0 EXPERIMENTAL SETUP	3
2.1 Equipment	3
2.2 Test Conditions	4
2.3 Processing Considerations	6
2.3.1 IQ Processing	6
2.3.2 Antenna Array Equalization	6
2.3.3 DF Estimation	7
3.0 OBSERVATIONS	9
4.0 SOURCES OF BEARING ERROR	18
4.1 Array Orientation	18
4.2 Wind Effect	18
4.3 Ideal Manifold Assumption	19
4.4 Receiver Drift	20
4.5 GPS Errors	20
4.6 Timing Errors	20
4.7 Noise	21
4.8 Reflections Off the Water Surface	21
4.9 Atmospheric Effects	22
5.0 CONCLUSIONS	24
REFERENCES	REF-1
A.0 An Antenna Array Equalization Method	A-1

LIST OF FIGURES

		Page
Figure 1:	GPS derived transmitter positions for October 24th and 25th	5
Figure 2:	Signal bearing and SNR measurements taken on October 24, 1995 at 10:07	10
Figure 3:	Signal bearing and SNR measurements taken on October 24, 1995 at 10:19	11
Figure 4:	Signal bearing and SNR measurements taken on October 25, 1995 at 10:33	12
Figure 5:	Signal bearing and SNR measurements taken on October 24, 1995 at 11:05	13
Figure 6:	DF results for October 24	14
Figure 7:	DF results for October 25	15
Figure 8:	Received signal power versus range for selected measurements on October 24	17
Figure 9:	Antenna array manifold error	19
Figure 10:	Theoretical effect of noise on bearing error versus actual results . . .	22

LIST OF TABLES

		Page
Table 1:	Sources of Bearing Errors during the Field Trials	18

1.0 INTRODUCTION

Electronic Support Measures (ESM) equipment operating against radar targets plays an important role in modern surveillance systems and platform protection systems. Advances in modern high speed signal processing technology have made numerous new features, which were previously impractical, now practical.

High accuracy radar direction finding (DF) is one such feature. Two important advantages in adding this feature to an ESM system are the improvement in the identification process and the addition of a geolocation capability. For identification purposes, the DF information can be used to improve the de-interleaving of radar pulses in a dense radar environment leading to higher accuracy in the identification of threat radars, or reduced processing time. Against high speed airborne threats, accuracy and response time are critical ingredients for survival.

For geolocation using the ESM system, a DF capability is essential. Based on the DF measurements, two or more ESM platforms can be used to triangulate the position of a target radar platform. Alternately, a single fast moving (airborne) platform can be used to triangulate the target by making use of successive DF measurements of the same radar. A further advantage is that, given the passive nature of the ESM sensor array, the geolocation can be done covertly. The ESM approach is preferable, in this regard, to a surveillance radar which can also geolocate a target but emits a train of RF pulses providing hostile forces with an opportunity to detect, geolocate, and determine the intentions of the platform.

Given these reasons, research and development work has been carried out at the Defence Research Establishment Ottawa (DREO) to investigate the issues involved with incorporating a high accuracy DF capability into an ESM system. As part of this work, an investigation has been undertaken to determine the effects of the environment on radar DF accuracy. To this end, the work reported here focuses on radar DF trials carried out to investigate the effects of the maritime propagation environment on the accuracy of measuring the azimuth angle-of-arrival of a radar signal.

These field trials took place in October 1995 at Osborne Head Gunnery Range near Halifax on Canada's East coast, and were part of a much larger collaborative set of field trials involving both DREO and the Defence Research Establishment Valcartier (DREV). Participation by DREO included experiments designed to investigate a variety of active

areas in radar research including adaptive array processing for jammer cancellation, low elevation tracking, rain and sea clutter measurements, as well as radar direction finding. Participation by DREV included experiments which were electro-optic in nature and were designed to study IR-visible refraction effects, and atmospheric remote sensing. This report details the radar DF portion of the trials.

2.0 EXPERIMENTAL SETUP

2.1 Equipment

For all the radar DF measurements, the Experimental Array Radar System (EARS) was used for collection purposes. EARS is a 16 channel system utilizing a vertical linear array of 8 radar horns with 12.5 cm spacing and a horizontal linear array of 8 radar horns with 6 cm spacing. Each horn feeds its own receiver which downconverts the signal from RF (8.9-9.4 GHz) to a final IF of 5 MHz with a bandwidth of 5 MHz. The 16 outputs are digitized at 20 MHz by a 16 channel digitizer into a real data stream. The digital data is initially stored in a 4 MB RAM memory buffer, then offloaded to a 13 GB disk array. At the end of an experimental day, the data from the disk array is transferred to tape for permanent storage and for later offline processing.

EARS was designed as a radar system. Operating as such, data collection is based on the known pulse repetition frequency (PRF) of the emitted radar signal and the approximate range of the target. With these parameters, signal collection can be set to cover only those intervals of time when a returned radar pulse may actually be present in the measurements. Allowed to run continuously, the collected data would quickly overrun the memory.

To use EARS in a DF application, certain adaptions had to be made. For one, the radar transmitter was left off, effectively turning EARS into a 16 channel radar ESM receiver. Since the receiver has no capability to synchronize with an external RF pulse, a CW transmitter was used as the target source. In this way, regardless of when data was collected and assuming propagation conditions permitted, a signal would always be present. The system was then set up to collect data as if the radar transmitter was on and operating at the same frequency as the CW source with a PRF of 500 Hz and with the target located between 2 and 4 km. This corresponds to a collection of 264 samples per channel every 1/500th of a second. To limit the total amount of data, collections were normally limited to 10-second intervals repeated every 2 minutes.

EARS was mounted on a turntable to allow it to be aimed at the desired target. A scale at the base of the turntable, graduated in 1 degree increments, was used to provided the current antenna heading information. For DF purposes, the system was generally left in one position. When moved, the new orientation was recorded for later incorporation into the DF estimates.

Only a single CW target was used throughout the DF measurements. It consisted of a portable radar jammer set up to produce a CW signal at 9.1 GHz. It was mounted onboard the ship the CFAV Riverton and accompanied by a technician who ensured that the transmitting horn was approximately aimed at EARS at all times, and replaced the transmitter batteries when required.

The position of the ship was monitored using a GPS receiver. A second GPS was located at the EARS site with the intention of performing differential GPS to get higher location accuracy of the transmitter. Unfortunately technical difficulties with the second GPS setup precluded it from being used for more than a few differential measurements, with the result that location accuracy was that of a single GPS receiver system.

2.2 Test Conditions

The Osborne Head Gunnery Range, where the field trials took place, is located on the coast of the Atlantic Ocean on the approach to Halifax Harbour. EARS was located at the top edge of a cliff overlooking the ocean. The height above mean sea level of the horizontal array in this location was 26.7 meters.

The radar DF measurements took place on Oct 24-25, 1995. During these two days the ship was directed along various paths which were either directly in line with EARS, or moving perpendicular to it. The GPS derived ship positions measured at 10-second intervals are shown for both days in Figure 1a and b. Each path is labelled by a separate letter. The time sequence of measurements is given by the order of the letter labels, and the direction of the arrows.

In addition to the above measurements, a 20-second DF measurement was taken on Oct 24 (marked by the letter B in Figure 1a) with the ship stationary and the EARS array turning. During this measurement, the array was turned through an angle of 38 degrees with the signal at boresight midway through the measurement. The purpose of the measurement was to provide some characterization of the array manifold.

The weather conditions during the two days varied. On the 24 of October the conditions were pleasant with virtually no clouds, light winds, and temperatures near 20C. Wave heights were approximately 1.1 meters with a periods of 8 seconds. On the 25th of October the sky was overcast with scattered showers and increasing winds. Temperatures were a few degrees cooler. Wave heights were 1.6 meters with periods of 5.5 seconds.

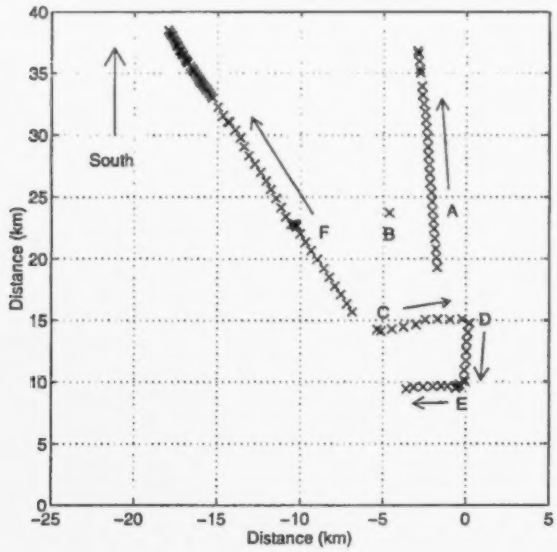

(a)

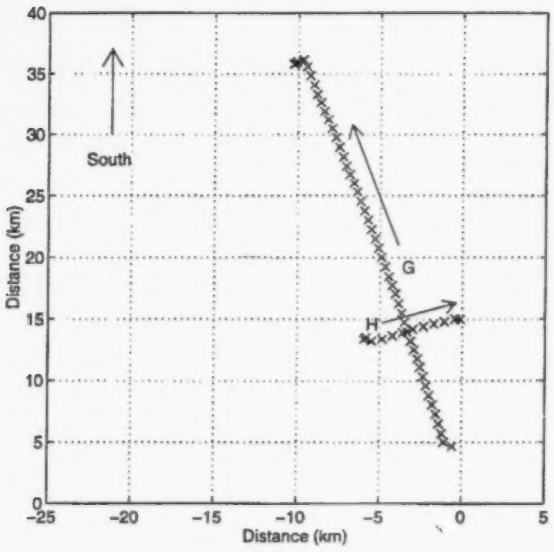

(b)

Figure 1: GPS derived transmitter positions for (a) October 24, 1995, and (b) October 25, 1995. EARS is located at the origin.

2.3 Processing Considerations

2.3.1 IQ Processing

The accurate knowledge of the signal frequency permits use of the discrete Fourier transform (DFT) to coherently integrate a block of M real data values to produce a single IQ value. The appropriate expression is given by

$$y_k = \sum_{m=0}^{M-1} x_k(m) e^{-j2\pi mf} \quad \text{for } k = 1, 2, ..., 16 \tag{1}$$

where y_k is the IQ value for channel k, $x_k(m)$ is the m^{th} real sample in the block of M for channel k, and f is the normalized frequency. The normalized frequency value is given by

$$f = \frac{f_o}{f_s} \tag{2}$$

where f_o is the frequency of the signal before sampling and f_s is the sampling frequency. If the above DFT approach is performed on successive blocks of data, it results in a decimation by a factor of M, i.e. L blocks of $16 \times N$ of real data is reduced to a block of $16 \times L$ complex data.

For the field trial data, processing was carried out using a channel block size of $M = 264$. The frequency of the signal before sampling was the final IF frequency, in this case, $f_o = 4.99$ MHz. Given a sampling rate of $f_s = 20$ MHz, this yielded the normalized frequency value of $f = 0.2495$ which was the value used for processing.

2.3.2 Antenna Array Equalization

Ideally, the measurement system would be equalized so that a plane wave from the boresight direction of the linear antenna array would yield exactly the same amplitude and phase across the array. In the context of the antenna array, "equalized" is used here to mean compensation of amplitude and phase error offsets introduced by the equipment.

Determining these amplitude and phase error offsets, which are usually unknown, can be somewhat problematic under real-world conditions. Using internally generated reference signals to measure these offsets generally ignores the affects of the receive antennas, while externally generated signals can incorporate the effects of multipath sources. Since

EARS has no provision for internally generated signals, however, the choice was limited to using an external approach.

To minimize the effects of multipath sources, a large number of measurements of the CW transmitter, covering as wide a range of bearing angles as possible, were pulled from the measurement data set. The theoretical data corresponding to the selected measurements was also generated using the known time of collection and the GPS-derived transmitter positions. For the theoretical data, the received signal was assumed to be a perfect planewave. Using the least squares techniques outlined in Appendix A, the unknown channel phase and gain offsets were estimated and the appropriate equalization coefficients determined. These equalization coefficients were then applied to the IQ data anytime DF estimates were to be made.

2.3.3 DF Estimation

To estimate the DF azimuth bearings, an interferometer approach was used on the data generated by the horizontal array. The approach used is based on deriving the direction of the signal based on the phase differences between antenna elements. For a horizontal uniform linear array, the relative phase differences are given by

$$\theta_k = \frac{2\pi}{\lambda}(k-1)d\sin\phi\cos\psi \quad \text{radians} \tag{3}$$

where θ_k is the phase of antenna k measured relative to antenna 1, d is the spacing between antennas, λ is the signal wavelength, ϕ is the azimuth angle of the transmitter measured clockwise from the boresight of the antenna array (at boresight $\phi = 0$), and ψ is the elevation angle measured upwards from the horizon (on the horizon $\psi = 0$). Given that during the trials $-0.4° < \psi < 0°$, the effect of elevation was insignificant so the phase expression can be simplified to

$$\theta_k = \frac{2\pi}{\lambda}(k-1)d\sin\phi \quad \text{radians} \tag{4}$$

To get the azimuth bearing estimate, any of the phase measurements can be used, but the best accuracy is achieved by using the phase measurement for the most widely separated antennas. Given K antennas in the horizontal array, then the azimuth angle

can be estimated using

$$\hat{\phi} = \sin^{-1}\left(\frac{\theta_K \lambda}{2\pi(K-1)d}\right) \tag{5}$$

A fundamental problem with linear arrays, which is reflected in this expression, is that it cannot be determined which of the two results $\hat{\phi}$ and $\pi - \hat{\phi}$ is correct, i.e. it is impossible to tell whether the signal is arriving from the front or the back of the array. A second problem is that phase differences between two antennas can only be determined within the range $-\pi$ to $+\pi$. If the smallest antenna spacing is constrained so that θ_1 does not exceed this range, then the phase differences for the smaller spacings can be used to unwrap the phase differences for the larger spacings (e.g. $\theta_2 = 2\theta_1$). However, if the minimum antenna spacing exceeds $\lambda/2$ then this phase unwrapping approach can fail. Thus, these two problems lead to ambiguities in the bearing estimates.

For the trials, the ambiguity problem was overcome by rotating the antenna array so that the transmitter target was always on the same side of the array (overcoming the first problem) and within $\pm 15^\circ$ of the array boresight (overcoming the second problem). The $\pm 15^\circ$ limit was selected in order to restrict the minimum phase difference to the range $-\pi < \theta_1 < +\pi$ for the horizontal array where the antenna spacing was 1.82λ at 9.1 GHz. The only exception to the $\pm 15^\circ$ limit was the 20-second manifold measurement. In this case, corrections to the phase were made by comparing the measured phases to (4) using the known orientation of the array with respect to the transmitter, and then adding the most appropriate increment $2n\pi$ where $n = 0, \pm 1, \pm 2, \ldots$ to the measured phase.

Once the raw bearings were estimated, an offset was added corresponding to the difference between the boresight of the array and true North. The corrected bearings were then compared to the GPS-derived bearings.

3.0 OBSERVATIONS

Figures 2-5 show representative examples of 10-second measurements which illustrate some of the short term temporal effects which occurred in the DF and signal-to-noise ratio (SNR) results. Each dot in these plots represent a single snapshot of data. The time gaps in the measurements were caused when the RAM memory buffer became full (this caused collection to be suspended until the contents of the RAM memory were copied to the disk array). Data loss also occurred near the end of each measurement interval possibly due to a software problem (the last second of data stored in RAM memory buffer did not appear to get dumped). Consequently in each 10-second interval, only 7.8 seconds of data (3879 snapshots) was actually collected. The GPS derived bearings are shown by the dashed lines. In most cases the measured DF bearings and the GPS bearings were within a few tenths of a degree of each other.

Inspection of these figures indicate that bearing errors were relatively small except when the SNR dropped to low levels. Since transmitter power levels were set to provide a high SNR at the receiver most of the time, the main instances of low SNR coincide with nulling (see Figure 3b at approximately 4 and 8 seconds). Both the relationship between SNR and DF accuracy, and the amplitude nulls, are discussed in more detail in Section 4.

To assess the overall accuracy, all the measurement data from October 24th and 25th were processed in the manner just described. Each 10-second sample was then averaged to give a single bearing. The GPS derived bearings were also determined corresponding to each 10-second interval. The results for each day are shown in Figures 6 and 7; these figures include both the estimated bearings and the bearing errors computed by subtracting the GPS-derived bearings from the bearings estimated using the EARS data.

As in the previous examples, the bearing errors were relatively small with an overall RMS error for the two days of measurements of 0.2 degrees. Errors up to ± 0.5 degrees occurred during intervals when the transmitter bearings were changing the fastest. This suggests that part of these errors was attributable to timing error (the EARS measurements were manually triggered and the corresponding times manually recorded).

Bearing errors of 0.6 degrees also occurred at the beginning of the measurements taken October 25th even though the transmitter bearing was changing very slowly. Since these measurements were taken with transmitter-receiver distances of less than 10 km, the 100

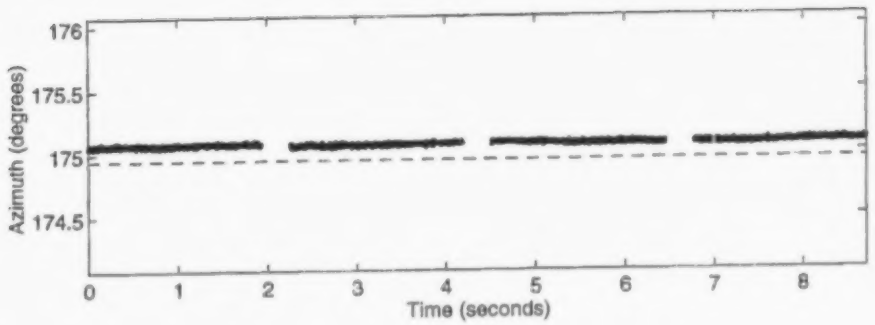

(a)

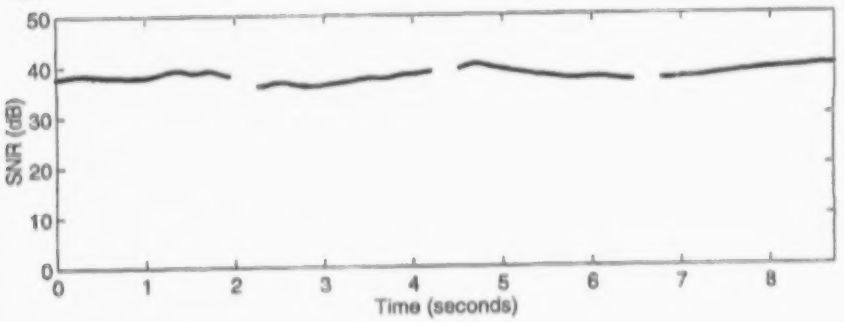

(b)

Figure 2: Measurements taken on October 24, 1995, at 10:07 (Path A) showing the (a) estimated bearing (GPS derived bearing is shown as the white dashed line) and (b) the corresponding received SNR.

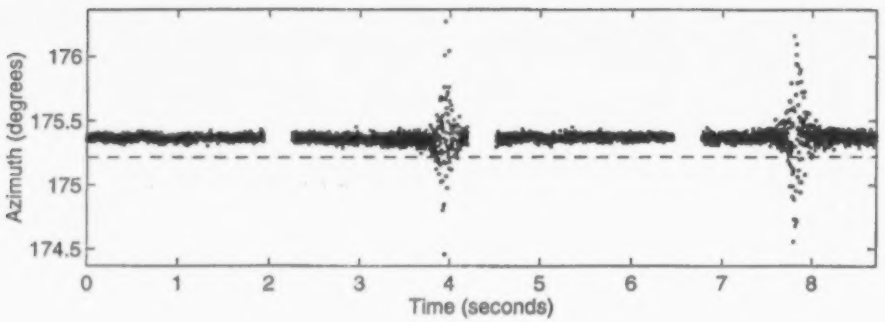

(a)

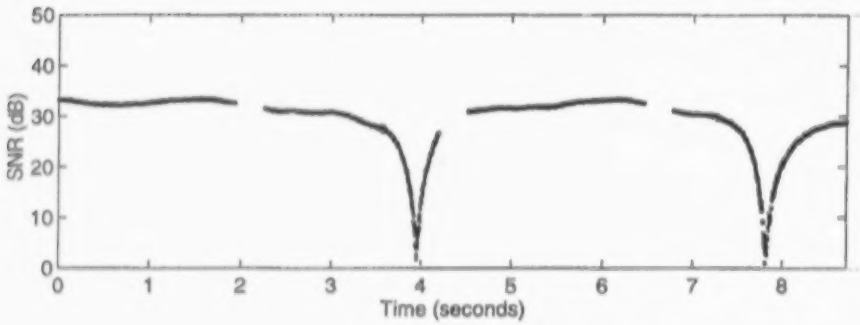

(b)

Figure 3: Measurements taken on October 24, 1995, at 10:19 (Path A) showing the (a) estimated bearing (GPS derived bearing is shown as the white dashed line) and (b) the corresponding received SNR.

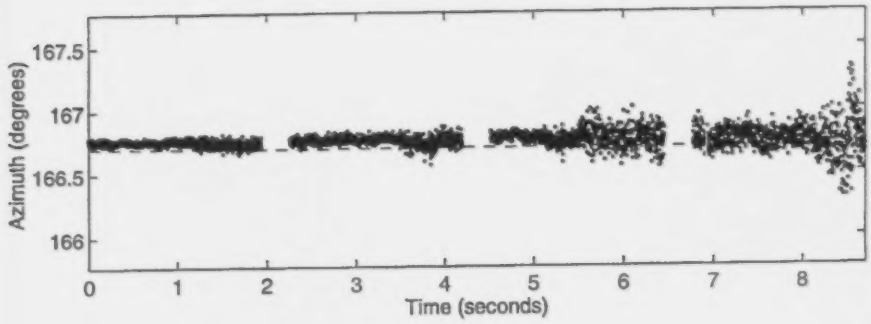

(a)

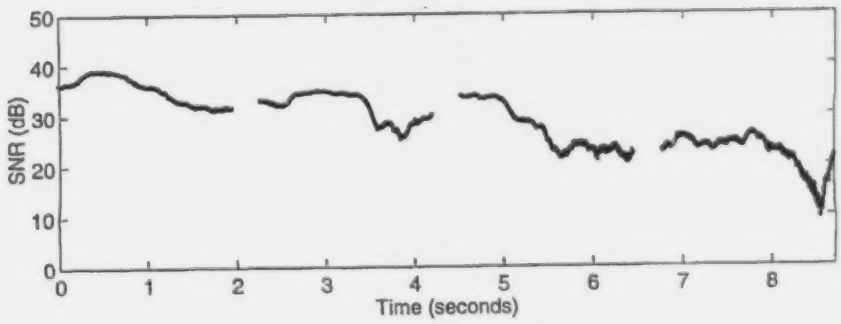

(b)

Figure 4: Measurements taken on October 25, 1995, at 10:33 (Path G) showing the (a) estimated bearing (GPS derived bearing is shown as the white dashed line) and (b) the corresponding received SNR.

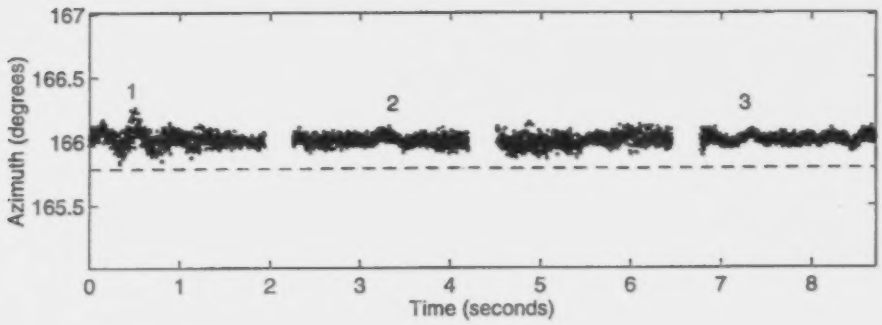

(a)

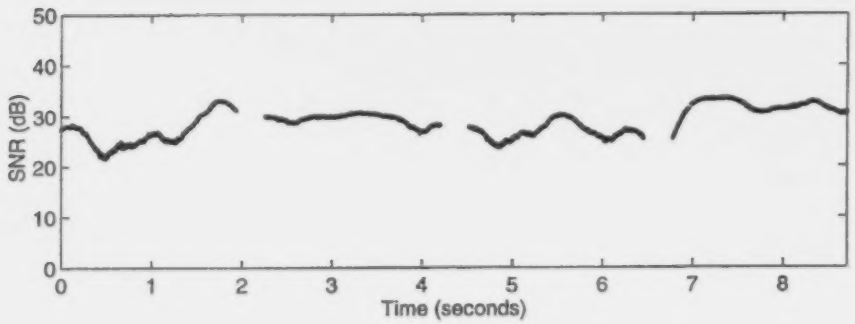

(b)

Figure 5: Measurements taken on October 25, 1995, at 11:05 (Path G) showing the (a) estimated bearing with small oscillations labelled by numbers (GPS derived bearing is shown as the white dashed line) and (b) the corresponding received SNR.

meter position accuracy of the GPS measurements was certainly a factor.

Timing and GPS position errors were probably the most obvious sources of bearing error, and probably accounted for most of the larger errors. These sources of errors are discussed in detail and quantified in the next section, along with all other known sources of error.

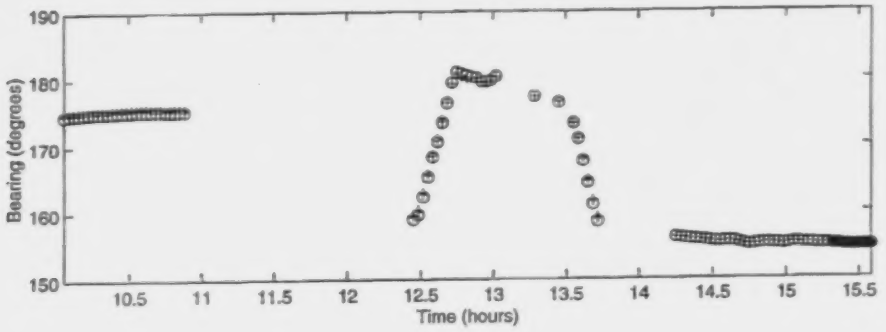

(a)

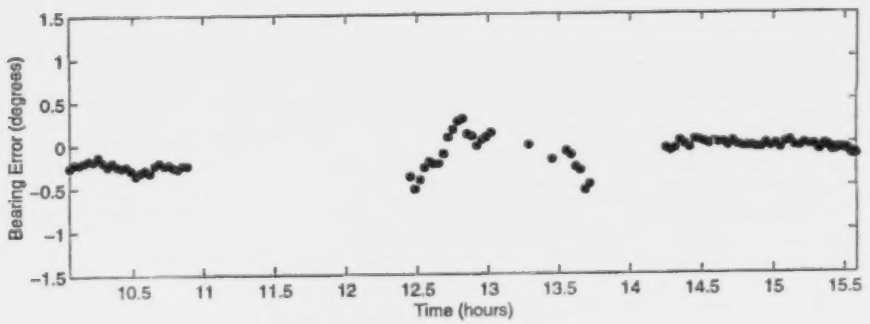

(b)

Figure 6: DF results for October 24 showing the (a) estimated bearings using EARS (o) and GPS (+), and (b) the estimated bearing errors.

One other observation worth noting is the effect of the radio horizon which was located at 35.9 km (based on the heights of the CW and EARS antenna array, and assuming standard refraction). The final 33 measurements beginning at 15:19 on October 24th were made after the transmitter had passed this distance (see Figure 1a). The maximum range at which the transmitter was measured was 42.5 km. Since it has been observed that the performance of microwave radar systems rapidly degrade once the radio horizon has

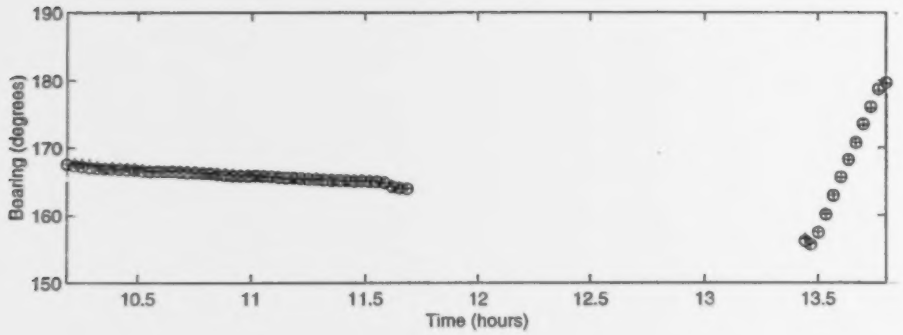

(a)

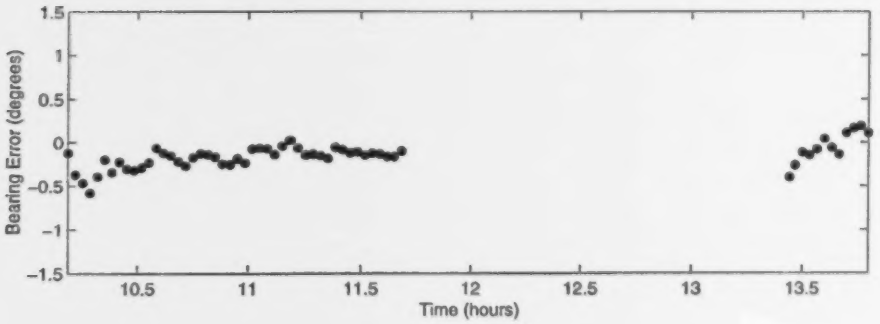

(b)

Figure 7: DF results for October 25 showing the (a) estimated bearings using EARS (o) and GPS (+), and (b) the estimated bearing errors.

been passed [3], it is useful to see whether DF performance is also degraded. Inspecting the DF measurements made at these ranges does not appear to reveal any obvious adverse effects (see Figure 6b and compare the scatter in the error results before and after the time 15:19).

To better quantify the effect of the horizon, the average power of the received signal for each 10-second interval beginning at 14:41 until the final measurement at 15:35 on October 24th was calculated, along with the corresponding range of the transmitter. The results are plotted shown in Figure 8. Generally the received signal power is observed to decrease with increasing range. From 25 km to the horizon, the decrease in power is approximately 2 dB. From the horizon out to 42.5 km, the decrease is much more rapid with a total drop of approximately 14 dB. Even with this excess loss of 14 dB, the resultant SNR of approximately 20 dB was still high enough to produce good DF results. Had the measurements been continued out to greater ranges, the SNR would likely have continued to drop off reaching 0 dB between 45 and 50 km with degraded DF performance the result.

Clearly then, as in the case of microwave radar, DF performance also degrades when the radar horizon is passed. However, since the propagation losses in the DF case are only one-way (versus two-way for the radar case) the degradation is less rapid. For example, under the same conditions used to produce the results in Figure 8, the excess loss for the radar case at 42.5 km would have been twice that of the DF case, or $2 \times 14 = 28$ dB.

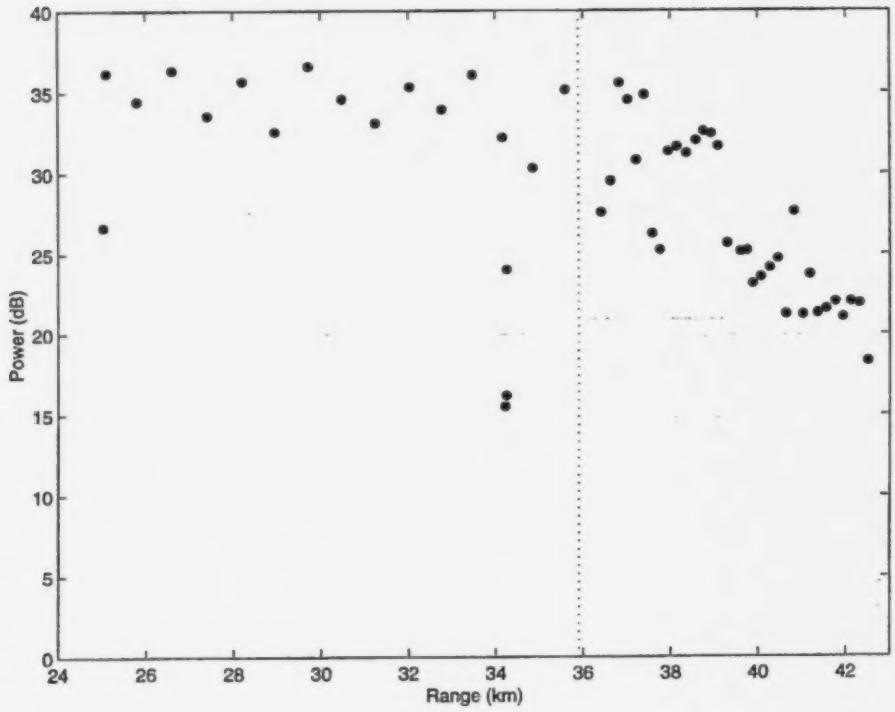

Figure 8: Received signal power versus range for selected measurements on October 24. The dotted line shows the location of the radio horizon.

4.0 SOURCES OF BEARING ERROR

All the known sources of the bearing errors observed in Figures 2-7 have been listed in Table 1, along with the estimated RMS error contributions for these sources.

Given the purpose of the DF trials, the propagation effects (last two entries in Table 1) were of the most interest. However, the contribution from these sources to the overall error was negligible with the exception of when reflections caused low signal-to-noise ratios (in which case it was the noise that caused the error). The most prominent source of error were due to the method of determining the actual location of the transmitter (GPS and timing errors) and noise. A detailed discussion of all of the error sources listed in Table 1 is provided in the following subsections.

Table 1: Sources of Bearing Errors during the Field Trials

Cause of Errors	RMS Error Contribution
Uncertainty in the array orientation	0.14°
Wind effects	$< 0.10^\circ$
Ideal array manifold assumption	0.08°
Receiver drift	0.08°
GPS location	$< 0.60^\circ$
Timing errors	$< 0.20^\circ$
Noise (internal and external)	$0.716^\circ/\sqrt{snr}$
Reflections off the sea surface	negligible
Atmospheric effects	negligible

4.1 Array Orientation

The uncertainty in array position was due to the fact that the array often had to be rotated for non-DF experiments. Using the scale on the turntable (marked in one degree increments) it was estimated that array orientation could be set to within ± 0.25 degrees of the desired direction. Assuming orientation errors were equally likely within this interval, this translates to an RMS error of 0.14 degrees.

4.2 Wind Effect

The wind effects discussed here relate to the uncertainty in the array position when a

strong wind causes the array structure to twist. This was a problem on October 25 when the array was twisted and rocked by strong winds. Inspection of the data has revealed that the wind had relatively little effect, although during periods when the wind was strongest, small sinusoidal oscillations were found in the DF estimates. Some examples are labelled 1, 2, and 3 in Figure 5a. There was very little evidence of these kinds of oscillations on October 24, when there was virtually no wind, The peak-to-peak magnitude of the oscillations was 0.3 degrees or less which equates to 0.1 degrees RMS.

4.3 Ideal Manifold Assumption

For DF estimation purposes, the array was assumed to act like an array of isotropic antennas with no mutual coupling between the antennas and no coupling with the supporting structure. This assumption was checked by comparing the assumed array phase output with the 20 second measurement from October 24 when the array was turned. Figure 9 shows the difference between the assumed value of θ_8 (the phase difference between the outermost antennas of the horizontal array) and the measured value. The RMS error in the assumed phase response was ± 6.6 degrees. This translates into a DF estimation error of 0.08 degrees RMS.

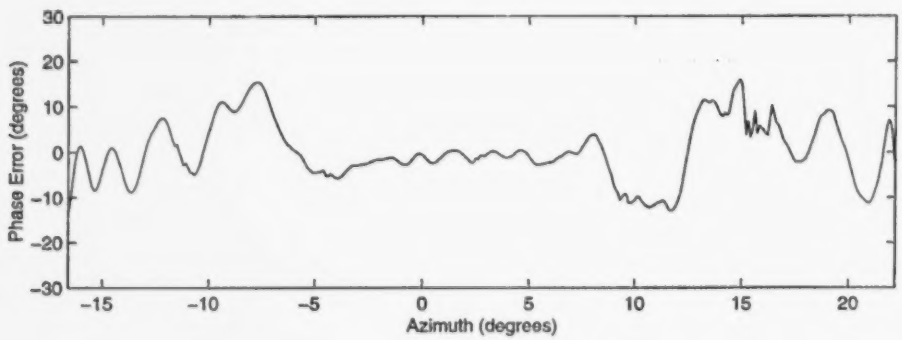

Figure 9: Error in the assumed phase response between the outermost antennas of the horizontal array.

Note that since the interferometer approach uses phase information only for the DF estimates, amplitude errors were ignored.

4.4 Receiver Drift

Phase and amplitude drift did occur in the receivers, particularly in the first few hours after EARS had been turned on. The relative phase drift between channels was determined to be ± 10 degrees. For the observed drift, the effect on the DF estimates was determined to be 0.05 degrees.

4.5 GPS Errors

During the Osborne trials, a GPS receiver on board the CFAV Riverton provided continuous GPS measurements (every 2 seconds), while a second GPS receiver at the EARS site provided sporadic GPS measurements. Since the fixed site measurements were too infrequent to perform differential GPS, the position accuracy was effectively that of a single GPS receiver system.

The specified position accuracy for a single receiver GPS system is 100 meters or less 95% of the time. This translates into an RMS position accuracy of 50 meters. The minimum range for the measurements was 5 km, and at this range the uncertainty in the bearings (calculated using the GPS position information) is 0.6 degrees RMS. For other ranges, a reasonable approximation is given by

$$RMS\ error = 2900/range \tag{6}$$

where *RMS error* is in degrees and *range* is in meters.

4.6 Timing Errors

The accuracy of the GPS measurements was also affected by the accuracy of the timing information for the EARS measurements. The EARS measurements were triggered manually at designated 2-minute or 30-second intervals. The error in triggering typically never exceeded 10 seconds. The effect of the timing error depends on the rate of change of bearing: it is negligible for a stationary target, and becomes more and more significant the faster the target bearing changes. The highest rate of change in the target bearing was 1.4 degrees/minute which occurred during the measurements marked by the letter "C" in Figure 1. Using this as the worst case, then for a 10-second timing error the equivalent bearing error would have been 0.2 degrees.

4.7 Noise

Noise, either generated in the receivers or generated externally places limitations on how accurately DF estimation can be performed. For a linear array the ultimate accuracy is defined by the Cramer-Rao bound which can be reasonably approximated by [1]

$$\sigma_\phi = \frac{90\sqrt{6}\lambda}{\pi^2 d|\cos\phi|\sqrt{snrN(N^2-1)}} \qquad (7)$$

where σ_ϕ is the standard deviation of the bearing errors in degrees, ϕ is the transmitter bearing, λ is the wavelength, d is the spacing between antenna elements, N is the number of elements, and snr is the SNR. Since the interferometer approach uses only the outermost antennas to achieve its accuracy (the inner antennas are used for phase unwrapping purposes), then $N = 2$ and $d = 7 \times 0.06 = 0.42m$. Additionally given a transmitter frequency of 9.1 GHz and the fact that most bearings were near broadside (i.e. $|\cos\phi| \approx 1$), this leads to

$$\sigma_\phi = 0.716 snr^{-\frac{1}{2}} \qquad (8)$$

The effect of noise can be illustrated using the azimuth data from Figure 4a and the SNR data from Figure 4b. Deriving the standard deviation results from these to figures, Figure 10 compares the predicted standard deviation (the Cramer-Rao bound) versus the estimated standard deviation. The estimated standard deviation was computed starting with the first block of 20 measurements of the azimuth data, then shifting the block five places and repeating (i.e. using measurements 1-20, then 6-25, then 11-30, etc., to make the standard deviation estimates).

Comparing the predicted results with the estimated results, there is very good agreement between the two. This good agreement provides strong evidence that over time spans of a few seconds or less noise was the dominant source of random error.

4.8 Reflections Off the Water Surface

In a maritime environment, the receiver signal will generally consist of a direct signal, and a signal reflected off the water. For very calm conditions, the water will act like a perfect reflector. As the conditions become rougher, the water will act more like a bumpy mirror. The existence of this reflected signal leads to two types of error.

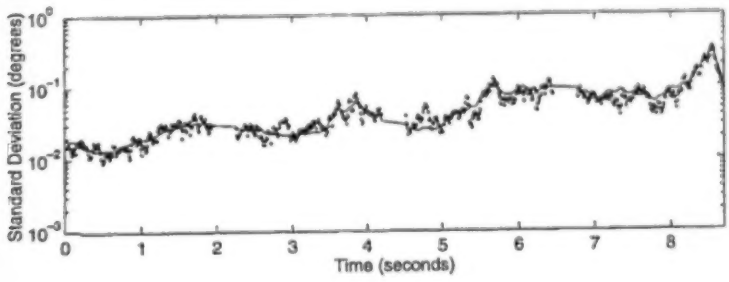

Figure 10: Theoretical effect of noise on bearing error (solid line) versus actual results.

The first type occurs when the direct and reflect signals are of similar amplitude but 180 degrees out-of-phase at the receiving array, so that a null occurs such as in Figure 3b. The corresponding drop in signal power then makes DF estimation more sensitive to noise effects.

Waves action may have also influenced the nulling by causing the boat carrying the transmitter to move up and down with the waves. For favourable geometries, the transmitter would then move into a null condition twice every wave cycle.

The second type, or rough surface effect, occurs as wave size grows resulting in specular and diffuse reflections from directions not in line with the direct signal, which causes an error in the DF estimate. Since waves move, the bearing errors will change over time. For measurements taken every two minutes, the effect on bearing would appear to be similar to that of noise. The main difference would be that bearing errors due to waves would not be effected by signal power, i.e. the rough surface effect would be more obvious at high SNR's. Examining Figures 6b and 7b, which were derived from data with high SNR's (particularly when the effect of averaging is taken into account), the errors varied slowly over time with very little indication of any random or noise-like error indicating that the rough surface effect was negligible.

4.9 Atmospheric Effects

Atmospheric effects also play a role. For example, subrefraction, superrefraction, and ducting conditions can modify how the signal is propagated from the transmitter to the receiver [3]. Since it is a more complex phenomena than the simple case of a direct and reflected signal, it might be expected that bearing estimation would be effected. Additionally, since the physical aspects of atmospheric phenomena are generally much

larger in scale and longer lasting than individual ocean waves, the resultant bearings errors would vary more slowly over time.

Examining the meteorological and electro-optical data collected during the trials, however, there were no indicators that any unusual atmospheric effects took place. Additionally, since the observed error could be adequately explained in terms of the other error sources, atmospheric conditions during the trials were deemed to be benign. Therefore the full effect of unusual atmospheric effects, based on these trials, remains unknown.

5.0 CONCLUSIONS

Based on an analysis of Osborne Head DF field trial data, accurate radar DF (significantly better than 1° RMS) can be achieved in a maritime environment. It was also found that signal losses rapidly increase beyond the radio horizon, but that high accuracy was still achievable for ranges several kilometers beyond the horizon. By comparison, radar performance more rapidly degrades at these ranges due to a doubling of these losses.

The conditions under which these accuracy assessment were made were: normal propagation conditions; a SNR of 20 dB or more; and a DF array 26.7 meters above the ocean surface. Altering these conditions does not necessarily invalidate the conclusions; however the effect of different conditions must be considered carefully. For example, performance as a function of SNR is well characterized and can be easily assessed for different levels. Atmospheric phenomena such as ducting may cause greater errors, however since no such phenomena occurred during the trials, the effect of this kind of phenomena could not be assessed. Lowering the DF antenna array would certainly enhance the effect of reflections and scattering of the signal off a rough sea surface in the vicinity of the antenna array. However, without further measurements, the height at which this effect becomes significant is unknown.

The main sources of bearing error during the trials were instrumental in nature. In particular, problems with one of two GPS receivers resulted in using a single GPS approach instead of the planned differential GPS approach. This change increased the expected GPS-derived bearing error from 0.05° to 0.3° RMS. Imprecise timing of the DF measurements may have also resulted in apparent errors of up to 0.2°.

The propagation effects which most obviously affected DF accuracy were nulling due to interference between the direct signal and the surface reflected signal. This seemed to be a relatively frequent occurrence, sometimes occurring every few seconds – a time span consistent with half the period of the ocean waves. For practical applications where only a few radar pulses are available for DF processing, this effect could pose serious difficulties if the measurements were taken during a null.

For completeness, future work should include an assessment of both DF antenna height and atmospheric phenomena (i.e. ducting) on the azimuth bearing accuracy of a radar DF system.

REFERENCES

[1] Read, W.J.L., "The Effects of the Environment on an Experimental VHF Radio Direction Finding Antenna System", DREO Report no. 1226, Ottawa, Canada, August 1994.

[2] Communication with Denis Dion, Defence Research Establishment Valcartier, October 1997.

[3] Skolink, M.I., "Introduction to Radar Systsems", Second Edition, McGraw-Hill Book Company, New York, U.S.A., 1980.

APPENDIX

A.0 An Antenna Array Equalization Method

In many practical radio direction finding (DF) problems, unknown phase and gain offsets are introduced by the local environment and the equipment including antennas, cables, connectors, and associated receiver electronics. Correcting for these unknown offsets is important for achieving accurate DF.

In this section, an array equalization method to correct for these errors is outlined. Note that the term "array equalization" has been used instead of "array calibration" since the phase and gain offsets are assumed to be independent of signal direction. The term "array calibration" is reserved for describing characterization of the array manifold, i.e. the antenna array response as a function of signal direction.

To start with, the $N \times T$ matrix $\mathbf{X}$ is used to describe a matrix of unequalized IQ data where N is the number of antennas in the array and T is the number of measurement snapshots. The T snapshots are chosen to represent as wide a range of transmitter directions as possible. The true direction of the transmitter for each snapshot is assumed to be known accurately (e.g. using GPS or a map), and each snapshot contains the measurement for only one transmitter. With this definition, channel equalization can be performed on the measured data $\mathbf{X}$ using the expression

$$\mathbf{Y} = \mathbf{A}^{-1}\mathbf{X} \tag{A.1}$$

$\mathbf{Y}$ is $N \times T$ matrix of equalized data representing the signals measured at the antennas, and $\mathbf{A}$ is an $N \times N$ diagonal matrix with complex gain elements $a_0, a_1, a_2, \ldots, a_{N-1}$. These complex elements can also be represented in terms of the real valued gain and phase, i.e. for channel k $(0 \leq k \leq N-1)$

$$a_k = g_k e^{\theta_k} \tag{A.2}$$

where g_k is the real-valued gain and θ_k the phase. Since g_k and θ_k are both relative terms, a_k will be ambiguous unless suitable references or constraints are chosen. To remedy this problem the phase is referenced to channel 0 so that

$$\theta_0 = 0 \tag{A.3}$$

and the gains are normalized so that

$$\sum_{k=0}^{N-1} g_k = N \tag{A.4}$$

Determination of the complex gain elements $a_0, a_1, \ldots, a_{N-1}$ is relatively straight forward if both $\mathbf{X}$ and $\mathbf{Y}$ are known. In reality $\mathbf{Y}$ will not be completely known and therefore must be estimated instead. This estimation requires a complete knowledge of the antenna array and the environment in which it is working. This includes the effects of temporal noise, mutual coupling, and the effects of multipath. Temporal noise can be minimized by performing the measurements at high SNR's (> 30 dB). Mutual coupling effects can be measured or modelled; they are ignored in this analysis, however. Errors introduced by multipath are assumed to be random with spatial white Gaussian characteristics and are treated in the same way as noise.

It follows from these assumptions that the equalized array response can be decomposed into a signal and a noise component as

$$\mathbf{Y} = \mathbf{A}^{-1}\mathbf{X} = \mathbf{SB} + \mathbf{N} \tag{A.5}$$

where $\mathbf{S}$ is the $N \times T$ signal matrix which is described in more detail below, $\mathbf{B}$ is a diagonal $T \times T$ matrix of complex signal amplitudes, also described below, and $\mathbf{N}$ is the $N \times T$ noise matrix which represents the error due to both temporal and spatial noise.

The signal matrix $\mathbf{S}$ can be defined in terms of its columns as

$$\mathbf{S} = [\mathbf{s}_0, \mathbf{s}_1, \mathbf{s}_2, \ldots, \mathbf{s}_{T-1}] \tag{A.6}$$

where $\mathbf{s}_0, \mathbf{s}_1, ..., \mathbf{s}_{T-1}$ are $N \times 1$ signal vectors normalized so that $|\mathbf{s}_k| = 1$ and the first element s_{k0} is real-valued for $0 \leq k \leq T-1$. Each signal vector represents the expected response of the antenna array to the signals measured during the corresponding snapshot assuming the array is equalized and there is no noise. If only a single signal is being

measured during each snapshot, and the antennas are omnidirectional, then

$$\mathbf{s}_k = \frac{1}{\sqrt{N}} \begin{bmatrix} 1 \\ e^{j\frac{2\pi d}{\lambda}\sin\phi_k} \\ e^{j\frac{4\pi d}{\lambda}\sin\phi_k} \\ \vdots \\ e^{j\frac{2(N-1)\pi d}{\lambda}\sin\phi_k} \end{bmatrix} \tag{A.7}$$

where d represents the spacing between antennas of the DF array, and $nd\sin\phi_k$ represents the path length difference between sensor n and sensor 0. The assumptions have also been made that the signal is a ground wave with an elevation angle of 0°, and that the shape of the wavefront is planar (i.e. the transmitter is in the farfield of the DF array, and mutual coupling and multipath effects are ignored). In the special case of a single signal, $\mathbf{s}_k$ is also called an *array steering vector.*

The matrix $\mathbf{B}$ is a diagonal matrix with diagonal elements $b_0, b_1, ..., b_{T-1}$. The element b_k represents the complex amplitude of the signal vector $\mathbf{s}_k$ in the k^{th} snapshot.

A solution for $\mathbf{A}$ and $\mathbf{B}$ in (A.5) could be determined by minimizing the total noise power given by trace($\mathbf{N}^H\mathbf{N}$). However, assuming that the dominant noise source is multipath, then the signal and multipath noise amplitudes will be correlated, i.e. the noise can be represented by

$$\mathbf{N} = \mathbf{WB} \tag{A.8}$$

where $\mathbf{W}$ is the normalized noise matrix – the multipath equivalent of the signal matrix $\mathbf{S}$. Since multipath is assumed to be spatial white Gaussian in nature, $\mathbf{S}$ and $\mathbf{W}$ will be uncorrelated and therefore a more optimum estimation of $\mathbf{A}$ and $\mathbf{B}$ can be achieved by minimizing the mean squared error function,

$$MSE = \text{trace}(\mathbf{W}^H\mathbf{W}) \tag{A.9}$$

where the normalized noise matrix $\mathbf{W}$ is found by substituting the right hand side of (A.8) into equation (A.5) and rearranging to get

$$\mathbf{W} = \mathbf{A}^{-1}\mathbf{X}\mathbf{B}^{-1} - \mathbf{S} \tag{A.10}$$

APPENDIX

A fundamental ambiguity exists with the above approach. The problem is that given the solution $\mathbf{A} = \mathbf{A_1}$ and $\mathbf{B} = \mathbf{B_1}$ for the minimization of the *MSE*, then the solution $\mathbf{A} = \kappa\mathbf{A_1}$ and $\mathbf{B} = \kappa^{-1}\mathbf{B_1}$ will also be valid. To remove this ambiguity, the complex gain coefficients are chosen so that

$$\text{imag}\{a_0\} = 0 \tag{A.11}$$

and

$$\sum_{k=0}^{N-1} |a_i|^2 = N \tag{A.12}$$

A closed form solution for determining $\mathbf{A}$ and $\mathbf{B}$ such that the *MSE* is minimized is unknown. The actual approach used to solve this problem was to minimize the *MSE* iteratively, first solving for $\mathbf{A}$ only, then solving for $\mathbf{B}$ only, and repeating. The advantage of this approach is that the separate minimizations involved have closed form solutions. For each successive iteration, $a_0, a_1, \ldots, a_{N-1}$ can be solved using,

$$a_i' = \frac{\sum_{n=0}^{T-1} p_{in} p_{in}^*}{\sum_{n=0}^{T-1} s_{in} p_{in}^*} \tag{A.13}$$

for $0 \leq i \leq N-1$ where a_i' is the unnormalized estimate of a_i, p_{in} and s_{in} are elements of the matrices $\mathbf{P}$ and $\mathbf{S}$ respectively, and

$$\mathbf{P} = \mathbf{X}\mathbf{B}^{-1} \tag{A.14}$$

The complex gain coefficients are then normalized so that

$$a_i = \frac{|a_0'| a_i'}{a_0'} \sqrt{\frac{N}{\sum_{i=0}^{N-1} |a_i'|^2}} \tag{A.15}$$

Similarly the parameters $b_0, b_1, \ldots, b_{T-1}$ can be solved each iteration using,

$$b_k = \frac{\sum_{m=0}^{N-1} q_{mk} q_{mk}^*}{\sum_{m=0}^{N-1} s_{mk} q_{mk}^*} \tag{A.16}$$

for $k = 0, 1, \ldots, T-1$ where q_{mk} is an element of the matrix $\mathbf{Q}$ which is given by,

$$\mathbf{Q} = \mathbf{A}^{-1}\mathbf{X} \tag{A.17}$$

APPENDIX

The minimization process is started by initializing the diagonal elements of **B** according to

$$b_k = \sqrt{\mathbf{x}(t_k)^H \mathbf{x}(t_k)} \tag{A.18}$$

and then for each iteration, updating the elements of **A** followed by the elements of **B**, according to equations (A.13)–(A.17). In practice, ten iterations has been found to ensure good convergence.

DOCUMENT CONTROL DATA

(Security classification of title, body of abstract and indexing annotation must be entered when the overall document is classified)

1. ORIGINATOR (the name and address of the organization preparing the document. Organizations for whom the document was prepared, e.g. Establishment sponsoring a contractor's report, or tasking agency, are entered in section 8.)

DEFENCE RESEARCH ESTABLISHMENT OTTAWA
DEPARTMENT OF NATIONAL DEFENCE
OTTAWA, ONTARIO K1A 0Z4

2. SECURITY CLASSIFICATION (overall security classification of the document including special warning terms if applicable)

UNCLASSIFIED

3. TITLE (the complete document title as indicated on the title page. Its classification should be indicated by the appropriate abbreviation (S,C or U) in parentheses after the title.)

RESULTS FROM THE RADAR DIRECTION FINDING TRIALS HELD AT OSBORNE HEAD IN 1995 (U)

4. AUTHORS (Last name, first name, middle initial)

READ, WILLIAM, J.L.

5. DATE OF PUBLICATION (month and year of publication of document)

JUNE 1998

6a. NO. OF PAGES (total containing information. Include Annexes, Appendices, etc.)

30

6b. NO. OF REFS (total cited in document)

3

7. DESCRIPTIVE NOTES (the category of the document, e.g. technical report, technical note or memorandum. If appropriate, enter the type of report, e.g. interim, progress, summary, annual or final. Give the inclusive dates when a specific reporting period is covered.

DREO REPORT

8. SPONSORING ACTIVITY (the name of the department project office or laboratory sponsoring the research and development. Include the address.

Defence Research Establishment Ottawa
Department of National Defence
Ottawa, Ontario Canada K1A 0Z4

9a. PROJECT OR GRANT NO. (if appropriate, the applicable research and development project or grant number under which the document was written. Please specify whether project or grant)

5BQ11

9b. CONTRACT NO. (if appropriate, the applicable number under which the document was written)

10a. ORIGINATOR'S DOCUMENT NUMBER (the official document number by which the document is identified by the originating activity. This number must be unique to this document.)

DREO REPORT 1330

10b. OTHER DOCUMENT NOS. (Any other numbers which may be assigned this document either by the originator or by the sponsor)

11. DOCUMENT AVAILABILITY (any limitations on further dissemination of the document, other than those imposed by security classification)

(X) Unlimited distribution
( ) Distribution limited to defence departments and defence contractors; further distribution only as approved, releasable to NATO, TTCP countries only
( ) Distribution limited to defence departments and Canadian defence contractors; further distribution only as approved
( ) Distribution limited to government departments and agencies; further distribution only as approved
( ) Distribution limited to defence departments; further distribution only as approved
( ) Other (please specify)

12. DOCUMENT ANNOUNCEMENT (any limitation to the bibliographic announcement of this document. This will normally correspond to the Document Availability (11). however, where further distribution (beyond the audience specified in 11) is possible, a wider announcement audience may be selected.)

UNLIMITED

UNCLASSIFIED
SECURITY CLASSIFICATION OF FORM

13. **ABSTRACT** (a brief and factual summary of the document. It may also appear elsewhere in the body of the document itself. It is highly desirable that the abstract of classified documents be unclassified. Each paragraph of the abstract shall begin with an indication of the security classification of the information in the paragraph (unless the document itself is unclassified) represented as (S), (C), or (U). It is not necessary to include here abstracts in both official languages unless the text is bilingual).

(U) This report discusses the results of microwave radio direction finding (DF) experiments carried out using the horizontal linear antenna array of an experimental N-channel radar system. The main purpose of these experiments was to investigate the effect of the maritime propagation environment on DF performance for signal paths up to and beyond the radio horizon. As part of this investigation, a comprehensive error analysis was carried out to identify and quantify the most significant sources of bearing error. These sources were mainly instrumental in error although significant errors could also be produced as a result of destructive interference between the direct signal and the ocean surface reflected signal. Based on the error analysis, it was concluded that in a maritime environment, microwave direction finding accuracies of significantly better than one degree RMS are possible, even for paths several kilometers over the radio.

14. **KEYWORDS, DESCRIPTORS or IDENTIFIERS** (technically meaningful terms or short phrases that characterize a document and could be helpful in cataloguing the document. They should be selected so that no security classification is required. Identifiers, such as equipment model designation, trade name, military project code name, geographic location may also be included. If possible keywords should be selected from a published thesaurus. e.g. Thesaurus of Engineering and Scientific Terms (TEST) and that thesaurus-identified. If it is not possible to select indexing terms which are Unclassified, the classification of each should be indicated as with the title.)

MICROWAVE
RADAR
RADAR DIRECTION FINDING
INTERFEROMETER
ANTENNA ARRAY
RADIO TRANSMISSION
RADIO PROPAGATION